ELSEVIER

Biochimica et Biophysica Acta 1514 (2001) 303–317

BIOCHIMICA ET BIOPHYSICA ACTA
BBA

www.bba-direct.com

A growth factor antagonist as a targeting agent for sterically stabilized liposomes in human small cell lung cancer

João N. Moreira [a,b], Christian B. Hansen [a], Rogério Gaspar [b], Theresa M. Allen [a,*]

[a] *Department of Pharmacology, University of Alberta, Edmonton, AB, Canada T6G 2H7*
[b] *Faculty of Pharmacy and Center for Neurosciences, University of Coimbra, 3000 Coimbra, Portugal*

Received 10 April 2001; received in revised form 28 June 2001; accepted 3 July 2001

Abstract

The ability of a growth factor antagonist, [D-Arg^6,D-Trp^{7,9}-*N*^{me}Phe^8]-substance P(6–11), named antagonist G, to selectively target polyethylene glycol-grafted liposomes (known as sterically stabilized liposomes) to a human classical small cell lung cancer (SCLC) cell line, H69, was examined. Our results showed that radiolabeled antagonist G-targeted sterically stabilized liposomes (SLG) bound to H69 cells with higher avidity than free antagonist G and were internalized (reaching a maximum of 13 000 SLG/cell), mainly through a receptor-mediated process, likely involving clathrin-coated pits. This interaction was confirmed by confocal microscopy to be peptide- and cell-specific. Moreover, it was shown that SLG significantly improved the nuclear delivery of encapsulated doxorubicin to the target cells, increasing the cytotoxic activity of the drug over non-targeted liposomes. In mice, [^{125}I]tyraminylinulin-containing SLG were long circulating, with a half-life of 13 h. Use of peptides like antagonist G to promote binding and internalization of sterically stabilized liposomes, with their accompanying drug loads, i.e., anticancer drugs, genes or antisense oligonucleotides, into target cells has the potential to improve therapy of SCLC.

Keywords: Antagonist G; Targeting; Pegylated liposome; Doxorubicin; Cytotoxicity; Small cell lung cancer

Abbreviations: SCLC, small cell lung cancer; HSPC, fully hydrogenated soy phosphatidylcholine; PL, phospholipid; mPEG$_{2000}$-DSPE, methoxy(polyethylene glycol) (2000) distearoylphosphatidylethanolamine; CHOL, cholesterol; mAB, monoclonal antibody; DXR, doxorubicin; PDP-PEG$_{2000}$-DSPE, *N*-(3′-(pyridyldithio)propionoyl)amino-poly(ethylene glycol) (2000) distearoylphosphatidylethanolamine; DTT, dithiothreitol; EMCS, ε-maleimidocaproic acid *N*-hydroxysuccinimide ester; MES, 2-(*N*-morpholino)ethanesulfonic acid; SL, sterically stabilized liposomes; SLG, antagonist G-coupled sterically stabilized liposomes; SLP(1–9), substance P(1–9)-coupled sterically stabilized liposomes; MTT, 3-(4,5-dimethylthiazol-2-yl)2,5-diphenyltetrazolium bromide; DNase, deoxyribonuclease; FBS, fetal bovine serum; HPTS, 8-hydroxypyrene-1,3,6-trisulfonic acid, trisodium salt; [^{3}H]CHE, [1α,2α(n)-^{3}H]cholesteryl hexadecylether; TI, tyraminylinulin; HEPES, *N*-(2-hydroxyethyl)piperazine-*N*′-(2-ethanesulfonic acid); PBS, phosphate-buffered saline, pH 7.4; TEA, 10 mM triethanolamine, 0.25 M sucrose, 10 mM acetic acid, 1 mM ethylenediaminetetraacetic acid (pH 7.4); IC$_{50}$, inhibitory concentration for 50% cell growth; MRT, mean residence time; $T_{1/2}$, elimination half-life; AUC, area under the blood concentration versus time curve; k_{10}, elimination rate constant from the central compartment

* Corresponding author. Fax: +1-780-492-8078. *E-mail address:* terry.allen@ualberta.ca (T.M. Allen).

0005-2736/01/$ – see front matter
PII: S0005-2736(01)00386-8

1. Introduction

Lung cancer is the most common fatal disease in the developed world [1]. Small cell lung cancer (SCLC) is a highly metastatic neuroendocrine tumor [2] that accounts for 25% of all pulmonary cancers and, despite an initial responsiveness to radiotherapy and chemotherapy, it progresses rapidly with a 5-year survival rate of less than 5% [3]. Hence, new therapies are urgently needed. SCLC cells are known to secrete multiple neuropeptides, whose binding to specific receptors triggers a cascade of intracellular signals culminating in DNA synthesis and cell proliferation [4]. This has led to the development of antagonists that block the mitogenic effects of neuropeptide growth factors [5–7]. Among these, the hexapeptide analogue of the neurotransmitter substance P, [D-Arg^{6},D-Trp^{7,9}-N^{me}Phe^{8}]-substance P(6–11), known as antagonist G, has gained special relevance. Antagonist G is a broad spectrum antagonist, that competitively blocks the action of multiple neuropeptides (e.g., vasopressin, gastrin-releasing peptide, bradykinin) through its ability to bind to several receptors on the surface of SCLC cells [6,8]. Recently, it has been demonstrated that antagonist G also induces apoptosis in SCLC via an oxidant-dependent mechanism [1]. Although antagonist G is sensitive to enzymatic degradation [9,10], and has a short half-life and a high volume of distribution in vivo [11], it can inhibit the growth of SCLC in vitro and in vivo [4,6,12] and is entering phase II clinical trials for the treatment of SCLC [1]. Antagonist G is a good example of the new generation of therapeutics that we can expect in the future. However, at present, chemotherapy along with radiotherapy is still the major treatment modality [13].

Ideally, anti-proliferative pharmaceuticals should have a high degree of selective toxicity, i.e., they should be specifically delivered to their target site(s) in order to achieve a high level of therapeutic efficacy and a low level of adverse effects. One means that has been used to increase the selective toxicity of anticancer drugs is encapsulation in liposomes. Association of drugs with small unilamellar polyethylene glycol (PEG)-grafted liposomes (known as sterically stabilized or Stealth liposomes), composed of high-phase transition phospholipids (PL) and cholesterol (CHOL) can significantly alter the pharmacokinetics and biodistribution of the drugs, resulting in increased tumor drug accumulation [14,15]. Since PEG-grafted liposomes are less susceptible to reticuloendothelial system uptake [16], they have increased plasma half-lives relative to liposomes lacking the PEG coating [17–19]. The long circulation half-lives of the PEG-liposomal drugs, along with their small size, leads to their differential accumulation in tissues with increased vascular permeability (e.g., tumors undergoing angiogenesis) relative to normal tissues, contributing to increased therapeutic efficacy relative to standard drug therapy [14]. Stealth liposomal doxorubicin (DXR) has received clinical approval for the treatment of Kaposi's sarcoma [20] and ovarian cancer [21].

Further improvements in the selective toxicity of anti-proliferative drugs might be achieved by coupling ligands selective for the target cell to the liposome surface. Methods have been developed for coupling ligands, directed towards internalizing receptors, at the end of PEG-grafted liposomes [22,23], resulting in improvements in the selective intracellular delivery of drugs to target cells [24–27]. Several studies with PEG-liposomal DXR targeted with monoclonal antibodies (mAb) have shown improved therapeutic activity over non-targeted formulations [28,29]. MAb-targeted liposomes have recently been used to deliver DNA [30] and antisense oligonucleotides [31]. However, the use of monoclonal antibodies as targeting ligands can be limited by their size, expense of production and potential immunogenicity [32]. Small molecules, e.g., peptides, carbohydrates or antibody fragments, may ultimately be better targeting agents. Recently, Fab′ fragments of the fully humanized version of the murine monoclonal antibody 4D5, directed against the glycoprotein p185^{HER2}, were used to target PEG-grafted liposomal DXR towards HER2-overexpressing human breast cancer cells. It was shown that the intracellular delivery of DXR was improved over non-targeted formulations [33], resulting in increased cytotoxicity [34] and tumor regression [35]. The affinity of antagonist G for several receptors on the surface of SCLC cells suggests that it is an attractive candidate for use as a ligand to target liposomal drugs in the treatment of SCLC. Small peptides have the advantage of being chemically defined and able to be manufactured in

large quantities in pure form, without biological contaminants.

Here, we investigated some of the mechanisms of interaction between antagonist G-targeted liposomes and the human SCLC H69 cell line. The effect of antagonist G-targeted liposomal DXR versus that of non-targeted formulations on the level of intracellular drug delivery and cytotoxic activity were compared. In addition, the pharmacokinetic and biodistribution profiles of antagonist G-targeted liposomes in mice were also examined. To the authors' knowledge, this is the first description of peptide-mediated targeting of liposomal drugs to SCLC.

2. Material and methods

2.1. Materials

Antagonist G and substance P(1–9), H-Arg-Pro-Lys-Pro-Gln-Gln-Phe-Phe-Gly-NH_2, were synthesized by Alberta Peptide Institute (Edmonton, AB). Fully hydrogenated soy phosphatidylcholine (HSPC), methoxy (polyethylene glycol) (2000) distearoylphosphatidyl-ethanolamine ($mPEG_{2000}$-DSPE) and *N*-(3′-(pyridyldithio)propionoyl)amino-poly(ethylene glycol) (2000) distearoylphosphatidyl-ethanolamine (PDP-PEG_{2000}-DSPE) were generous gifts of Sequus Pharmaceuticals (Menlo Park, CA), now Alza Corp. (Mountain View, CA). The synthesis of PDP-PEG_{2000}-DSPE has been previously described [27]. CHOL was purchased from Avanti Polar Lipids (Alabaster, AL). Sephadex G-50 and Sepharose CL-4B were purchased from Pharmacia (Uppsala, Sweden). Dithiothreitol (DTT), ε-maleimidocaproic acid *N*-hydroxysuccinimide ester (EMCS), 2-(*N*-morpholino)ethanesulfonic acid (MES), cytochalasin B, *N*-ethylmaleimide, 3-(4,5-dimethylthiazol-2-yl)2,5-diphenyltetrazolium bromide (MTT), digitonin, $MgCl_2$ and deoxyribonuclease (DNase) I (type II) were purchased from Sigma Chemical Co. (St. Louis, MO). RPMI 1640, penicillin-streptomycin and fetal bovine serum (FBS) were purchased from Gibco BRL (Grand Island, NY). DXR and 8-hydroxypyrene-1,3,6-trisulfonic acid, trisodium salt (HPTS) were obtained from Faulding (Vaudreuil, QC) and Molecular Probes (Eugene, OR), respectively. [1α,2α(n)-^{3}H]Cholesteryl hexadecyl ether, 1.48–2.22 TBq/mmol (^{3}H-CHE) was purchased from Dupont New England Nuclear (Mississauga, ON). $Na^{125}I$ and ACS scintillation fluid were purchased from Amersham (Oakville, ON). Iodobeads were obtained from Pierce (Rockford, IL). Tyraminylinulin (TI) was synthesized and [^{125}I]tyraminylinulin was prepared as previously described [36]. All other chemicals were of analytical grade purity.

2.2. Cell lines

The human classical SCLC cell line NCI-H69 (ATCC HTB-119) and the Namalwa cell line (human B-cell lymphoma; ATCC CRL 1432) were purchased from the American Type Culture Collection and cultured in RPMI 1640 supplemented with 10% (v/v) heat-inactivated FBS, 100 U/ml penicillin, 100 μg/ml streptomycin (full medium) and maintained at 37°C in a humidified incubator (90% humidity) containing 5% CO_2. Cells were maintained within their exponential growth phase.

2.3. Preparation of liposomes

Liposomes were composed of HSPC/CHOL/$mPEG_{2000}$-DSPE/PDP-PEG_{2000}-DSPE at a 2:1:0.08:0.02 molar ratio (total PEG lipid was 5 mol% of phospholipid). For HPTS or [^{125}I]TI-loaded liposomes, the aqueous-space labels were added during liposome hydration (at 65°C), according to [37] and [38], respectively. The resulting multivesicular preparations were then extruded at 65°C sequentially through 0.2 down to 0.08 μm polycarbonate membranes (Nucleopore, Pleasanton, CA) using a Lipex extruder (Lipex Biomembranes, Vancouver, BC), to give vesicles averaging 100 nm in diameter [39], as determined by dynamic light scattering. DXR was loaded into liposomes via an ammonium sulfate gradient, adapted from [40]. Briefly, liposomes were hydrated at 20 mM phospholipid (PL) in 250 mM ammonium sulfate, pH 5.5, and extruded as previously described. The external buffer was exchanged by passing the liposomes down a Sephadex G-50 column, equilibrated with 100 mM sodium acetate, 70 mM NaCl buffer (pH 5.5). DXR was then incubated with liposomes for 1 h at 65°C. Unloaded DXR, if any, was separated on a Sephadex G-50 column

eluted in the appropriate buffer and the amount of DXR encapsulated in the liposomes was determined from its absorbance at 492 nm. The loading efficiency of DXR was greater than 95% and the liposomes routinely contained approximately 200 μg DXR/μmol PL.

To conjugate antagonist G to the extremities of the liposomal PEG chains, liposomes were incubated with DTT for 30 min at room temperature, in order to reduce the pyridyldithiol groups. DTT was then separated and the pH raised by passing the liposomes down a Sephadex G-50 column eluted with HEPES buffer, pH 6.5 (25 mM HEPES, 25 mM MES, 140 mM NaCl). The maleimide derivative of antagonist G, obtained by reacting antagonist G with EMCS at 1:1 molar ratio (in HEPES buffer, pH 6.5) for 30 min at room temperature [41], was then incubated overnight at room temperature with thiolated liposomes at 1:200 antagonist G/PL molar ratio. Activation and coupling of antagonist G to liposomes took place in silicon-coated glassware (Sigmacote, Sigma). Free thiol groups were quenched by incubation with an excess of *N*-ethylmaleimide for 30 min at room temperature. Unbound antagonist G and *N*-ethylmaleimide were removed by passing the liposomes over a Sepharose CL-4B column, equilibrated in HEPES buffer at pH 7.4 (25 mM HEPES, 140 mM NaCl). The amount of antagonist G on the liposomes was determined by fluorimetry at $\lambda_{em} = 330$ nm, $\lambda_{ex} = 288$ nm. The amount of coupled peptide was approximately 1 μg antagonist G/μmol PL. The same procedure was used to couple an irrelevant peptide, substance P(1–9).

Phospholipid concentration was determined from either the specific activity counts of [^{3}H]CHE tracer (using a Beckman LS-6800 Scintillation counter) or by the Bartlett colorimetric assay [42].

2.4. Cellular association of liposomes

H69 or Namalwa cells (a non-specific cell line, which does not bind antagonist G) were plated at 1×10^6 cells/well in Falcon 48-well plates (Becton Dickinson, Lincoln Park, NJ). Sterically stabilized liposomes, radiolabeled with cholesterylhexyldecylether ([^{3}H]CHE), with or without coupled antagonist G (SLG versus SL), or with coupled substance P(1–9) as a non-specific peptide control (SLP(1–9)) [43], were added to each well at concentrations of 0.1–0.8 mM PL and maintained at either 4°C, for 1 h, or 37°C, for 1–4 h, in a total volume of 0.2 ml. In experiments with endocytosis inhibitors, H69 cells were pre-incubated with 25 μg/ml cytochalasin B/well or 0.45 M sucrose/well at 37°C for 30 min, or with physiological buffer only, either at 4°C or 37°C. SLG were then added (0.8 mM PL/well) and incubated for another hour at 4°C or 37°C. In competition experiments, the cells were incubated with either free antagonist G (0–29 μg antagonist G/well, for 30 min at 4°C or 37°C) or antagonist G-coupled liposomes (0–0.6 μg antagonist G/well) or plain liposomes, for 30 min at 37°C, before [^{3}H]CHE-SLG (0.1 mM PL/well) were added. After incubation, the cells were washed three times with cold phosphate-buffered saline, pH 7.4 (PBS). The amount of liposomes associated with cells was calculated from the initial specific activity of [^{3}H]CHE-liposomes from scintillation counting and was expressed as nmol of PL/10^6 cells.

In some experiments, cells were plated at 2×10^6 cells/well in 24-well plates (Nalge Nunc International, USA). HPTS-containing liposomes, with or without coupled antagonist G, were added to each well (0.8 mM PL/well, total volume of 0.4 ml) and maintained at 37°C in an atmosphere of 95% humidity and 5% CO_2 for 1 h. After washing the cells three times with PBS, the cells were visualized with a LSM-510 laser-scanning confocal microscope (Carl Zeiss), using an ultraviolet laser with emission at 364 nm for scanning. Cells were optically sectioned and images (512×512 pixel) were acquired using the LSM-510 software. All instrumental parameters pertaining to fluorescence detection and images analyses were held constant to allow sample comparison.

2.5. Cellular association kinetics of DXR

DXR cellular uptake kinetics were examined for the H69 cells as a function of time (0, 2, 6, 12 and 24 h), both in whole cell extracts and in isolated nuclei, using an adaptation of a previously described method [44]. Briefly, cells were seeded in 600 ml angled neck flasks (Nalge Nunc International) at 50×10^6 cells/flask. Free DXR or DXR-containing liposomes, with (DXR-SLG) or without coupled antagonist G (DXR-SL), or coupled with a non-specific

peptide (DXR-SLP(1–9)), were added at 20 μM DXR/flask, in a total volume of 100 ml/flask (one flask/time point). The cells were incubated at 37°C in an atmosphere of 95% humidity and 5% CO_2. At each time point, the cells from one flask were washed with 20 ml of 10 mM triethanolamine, 0.25 M sucrose, 10 mM acetic acid, 1 mM ethylenediaminetetraacetic acid, pH 7.4 (TEA) and resuspended in 4 ml TEA. Aliquots of 0.1 ml of cells were taken and diluted with 0.54 ml TEA to quantitate the levels of DXR in whole cells. The remaining cells were ruptured with two cycles of 25 firm strokes using a tight-fitting homogenizer on ice. The cell-free extract containing the nuclei was carefully removed from the cell pellet. Unbroken cells were submitted again to the same procedure. The two cell-free extracts were combined and spun at 2000 rpm for 2.5 min at 4°C to collect the nuclear pellet, which was further resuspended in 1 ml of TEA. Samples (0.2 ml) of either whole cells or nuclei were digested in the presence of 1.3 ml of TEA buffer, 0.01 ml 25 mg/ml digitonin, 0.01 ml 57 mg/ml $MgCl_2$ and 0.05 ml 3 mg/ml DNase I for 2 h at room temperature. Following digestion, the DXR fluorescence was determined at $\lambda_{em} = 595$ nm, $\lambda_{ex} = 480$ nm. Background was subtracted from the values in each time point and the results were expressed as DXR fluorescence units/50×10^6 cells.

2.6. Cytotoxicity experiments

In vitro cytotoxicity of free DXR or various DXR-containing liposomal formulations was determined for H69 cells or Namalwa cells (non-specific cell line) using the MTT proliferation assay [45]. Briefly, 8×10^4 H69 cells or 3×10^4 Namalwa cells were plated in 96-well plates (Costar, Corning, NY) and incubated with free DXR, DXR-SL or DXR-SLG. Additional controls included: free antagonist G, empty SLG or free DXR mixed with empty SLG (at 200 μg DXR/μmol PL). The cells were incubated for 2, 24 or 48 h at 37°C in an atmosphere of 95% humidity and 5% CO_2. At the end of the incubation, the cells were gently washed twice with PBS to remove drug. The cells were then maintained in fresh medium at 37°C in an atmosphere of 95% humidity and 5% CO_2, for up to 5 days for H69 cells and for 2 days for Namalwa cells. During the experiment, both cell lines were kept within their exponential growth phase. After incubation, the medium in each well was replaced by 50 μl 0.5 mg MTT/ml RPMI 1640 and the mixture was incubated at 37°C in an atmosphere of 95% humidity and 5% CO_2 for 4 h. Acid-isopropanol was added to each well (0.1 ml of 40 mM HCl in isopropanol) and mixed thoroughly until all crystals were dissolved. The plates were read immediately on a Titerk Multiskan PLUS MK II plate reader (Flow Laboratories, Mississauga, ON) using a test wavelength of 570 nm and a reference wavelength of 650 nm. IC_{50}s (μM of DXR, unless otherwise stated) were determined from the dose–response curves.

Table 1
Cytotoxicity of various formulations of DXR against H69 or Namalwa cells

Time (h)	DXR-SL	DXR-SLG	DXR	DXR+empty SLG	Empty SLG (μM PL)	Free antagonist G (μM antagonist G)
SCLC H69						
2	>200	9.59 ± 1.33	2.46 ± 0.93	2.28 ± 1.14	>1000	261 ± 64.3
24	161 ± 13.8	7.99 ± 4.33	0.68 ± 0.27	1.01 ± 0.45	>1000	135 ± 15.8
48	30.6 ± 11.8	3.35 ± 1.20	0.64 ± 0.28	0.82 ± 0.13	>1000	129 ± 7.42
Namalwa						
2	38.1 ± 9.19	33.9 ± 13.4	1.44 ± 0.19			
24	4.34 ± 1.65	4.04 ± 0.16	0.36 ± 0.03			
48	3.63 ± 1.46	1.95 ± 0.40	0.33 ± 0.03			

H69 cells (8×10^4/well) or Namalwa cells (3×10^4/well) were incubated with various treatments for 1, 24 and 48 h, after which the cells were washed and kept at 37°C in fresh medium for up to 5 days for H69 cells and for 2 days for Namalwa cells. Data are expressed as IC_{50} (μM of DXR, unless otherwise stated) and were extrapolated from the dose–response curves. The data represent the mean ± standard deviation of 3–8 independent experiments.

2.7. Pharmacokinetics and biodistribution of liposomes

The pharmacokinetics and biodistribution of both targeted and non-targeted liposomes, encapsulating [^{125}I]TI, were determined as previously described [27]. Pharmacokinetic parameters were calculated using polyexponential curve stripping and the least squares parameter estimation program PKAnalyst 1.0 (Micromath, Salt Lake City, UT). Biodistribution data were expressed as the percentage of counts in each organ relative to the total counts remaining in vivo at each time point.

2.8. Statistical analysis

Student's *t*-test was used to measure statistical significance. Multiple comparisons of IC_{50}s (Table 1) were performed using ANOVA. Data were considered significant at $P < 0.05$.

2. Results

2.1. Cellular association of liposomes

To determine whether the covalent attachment of antagonist G at the terminus of PEG would selectively target liposomes in vitro to SCLC cells, cellular

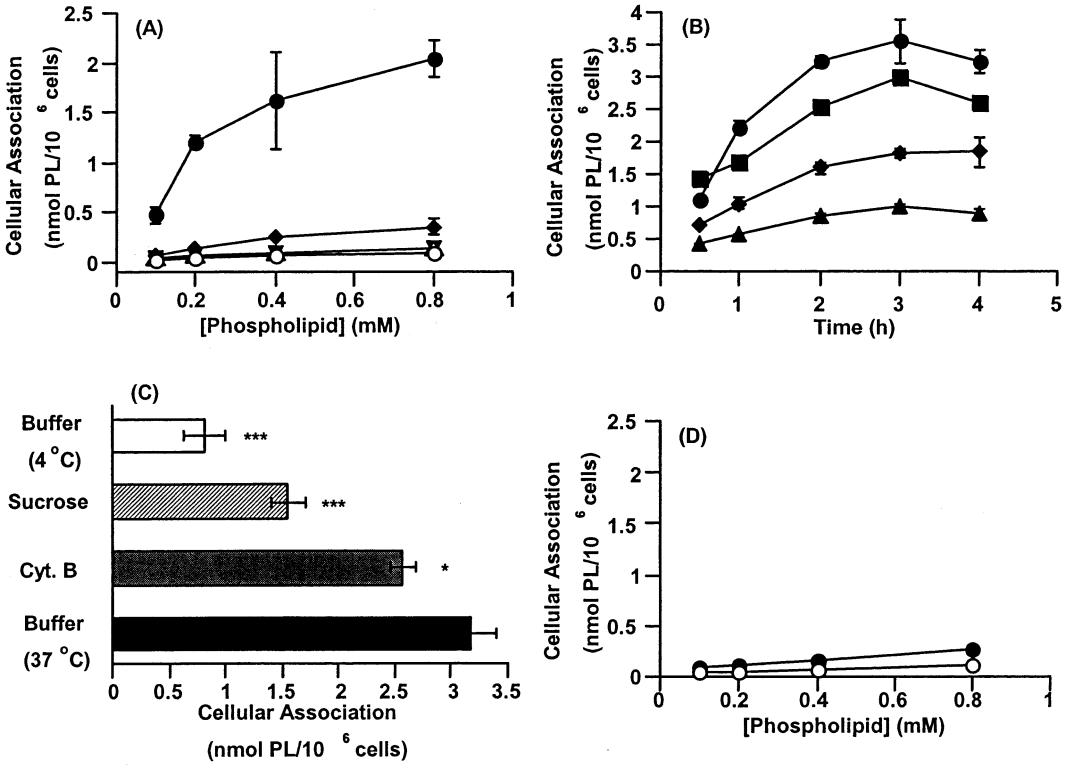

Fig. 1. Cellular association of several formulations of [^{3}H]CHE-labeled liposomes with SCLC H69 or Namalwa cells. Liposomes composed of HSPC/CHOL/mPEG$_{2000}$-DSPE/PDP-PEG$_{2000}$-DSPE at 2:1:0.08:0.02 molar ratio (0.1–0.8 mM PL/well) were incubated with 1×10^6 cells. (A) SCLC H69 cells incubated at 37°C for 1 h with SL (○), SLP(1–9) (▼), SLG at either at 4°C (♦) or 37°C (●), or SL in the presence of free antagonist G (△), at 1:200 antagonist G/PL molar ratio. (B) Time course of cell association of SLG with H69 cells incubated at different PL concentrations at 37°C for 4 h (0.1, ▲; 0.2, ♦; 0.4, ■; and 0.8 mM, ●). (C) H69 cells were preincubated at 37°C for 30 min with either 25 μg/ml cytochalasin B/well (dark-gray bar) or 0.45 M sucrose/well (light-gray bar), or in buffer only at either at 4°C (white bar) or 37°C (black bar). SLG were then added (0.8 mM PL/well) and samples were incubated for another hour at 4°C or 37°C. (D) Namalwa cells incubated with SL (○) or SLG (●) at 37°C for 1 h. After washing with cold PBS, the amount of [^{3}H]CHE-radiolabeled liposomes associated with cells was determined by scintillation counting and cell association of liposomes was calculated from the initial specific activity of [^{3}H]CHE. Data were expressed as nmol of PL/10^6 cells. Each point is the mean of 3–4 samples, ± standard deviation, from one representative experiment (*$P < 0.05$; ***$P < 0.001$).

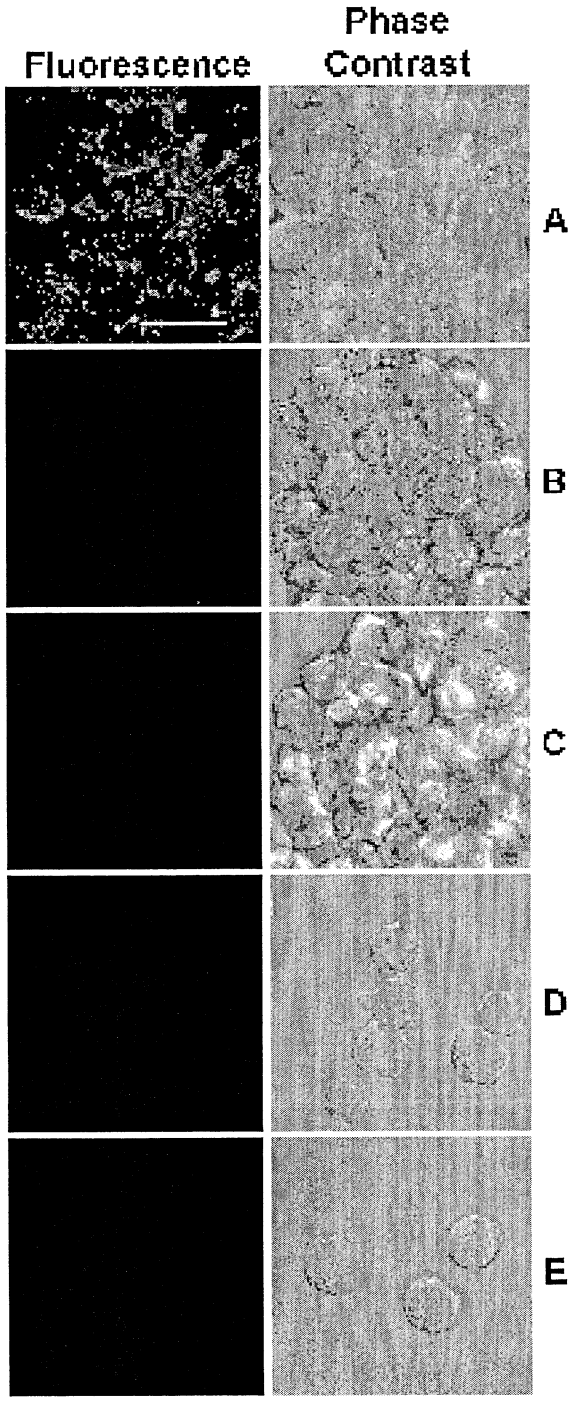

Fig. 2. Cellular association of HPTS-containing liposomes with H69 or Namalwa cells. Liposomes composed of HSPC/CHOL/mPEG$_{2000}$-DSPE/PDP-PEG$_{2000}$-DSPE at a 2:1:0.08:0.02 molar ratio (0.8 mM PL/well) were incubated with 2×10^6 cells at 37°C for 1 h. H69 cells were incubated with (A) SLG, (B) SL or (C) SLP(1–9). Namalwa cells were incubated with (D) SLG or (E) SL. After washing the cells with cold PBS, the cells were visualized with a LSM-510 laser-scanning confocal microscope. All instrumental parameters pertaining to fluorescence detection and image analyses were held constant to allow sample comparison. The results shown are from one representative experiment. Scale bar = 10 μm.

association experiments were carried out using the H69 and the negative control Namalwa cell lines. The term 'cellular association' is used to indicate a combination of binding on the cell surface plus cellular internalization of the liposomes together with their contents. To distinguish between binding plus non-specific cellular association and internalization, internalization of bound liposomes was inhibited by performing the experiments at 4°C, a temperature that is non-permissive for endocytosis [25]. At 37°C, the covalent attachment of antagonist G to PEG-liposomes increased both the amount and the rate of cellular association of SLG (21–37 fold) compared to either SL, SL in the presence of free antagonist G, or liposomes coupled to a non-specific peptide (SLP(1–9)) for H69 cells (Fig. 1A). This suggests that the association of SLG to H69 cells was peptide-specific.

The level of cellular association of SLG depended on the initial concentration of PL incubated with cells, and cellular association appeared to saturate above 0.8 mM PL (Fig. 1A). The maximum level of association was achieved after 2 h incubation and ranged from 0.9–3.3 nmol PL/10^6 cells (Fig. 1B). The substantial increase in the levels of association for SLG as the temperature was raised from non-permissive (4°C) to permissive temperatures (37°C) for endocytosis suggested that the SLG were being internalized (Fig. 1A).

Pre-treatment with 0.45 M sucrose (Fig. 1C), known to inhibit receptor-mediated endocytosis by blocking clathrin-coated pit formation [46], decreased the cellular association of SLG by 51% ($P<0.001$) at 37°C compared to the absence of endocytosis inhibitor. Pre-treatment with cytochalasin B (Fig. 1C), which blocks phagocytosis mediated by uncoated pits but not receptor-mediated endocytosis [47,48], decreased cellular association of SLG by only 19% ($P<0.05$). The sum of the decrease of internalization seen by sucrose plus the decrease by cytocha-

lasin B resulted in a total inhibition of 70%. The level of association under these conditions was similar to that observed for SLG at 4°C (Fig. 1C), where no internalization takes place [25].

Association of SLG with the control Namalwa cell line at 37°C was significantly lower (6–11 fold) than that seen for the H69 cell line (Fig. 1D vs. A). These data suggest that the covalent attachment of antagonist G to the terminal end of PEG-grafted liposomes leads to cell-specific cellular association of SLG.

Cellular association of SLG with the H69 cell line was further evaluated with several formulations of liposomes containing the fluorescent dye HPTS using laser-scanning confocal microscope (Fig. 2). After 1 h incubation, SLG were mainly distributed on the cell surface and in the cytoplasm (Fig. 2A). Under the same conditions, H69 cells incubated with SL (Fig. 2B) or SLP(1–9) (Fig. 2C) or Namalwa cells incubated with either SLG (Fig. 2D) or SL (Fig. 2E), had no detectable staining. These results were consistent both with the inability of liposomes without antagonist G to bind to and be internalized by H69 cells and with the absence of receptors on Namalwa cells that specifically recognize antagonist G.

Surprisingly, non-toxic concentrations (0–29 μg/well) of free antagonist G, pre-incubated for 30 min with 1×10^6 H69 cells, did not competitively inhibit the binding of [^{3}H]CHE-SLG, either at 37°C or at 4°C (Fig. 3A). However, when antagonist G was coupled to non-radiolabeled (i.e., cold) liposomes and pre-incubated with the H69 cells at 37°C, the cell binding of SLG was inhibited at low levels of liposome-coupled antagonist G, in a concentration-dependent manner. Fifty percent inhibition of cell binding was reached with 0.037 μg of liposome-coupled peptide. A maximum inhibition of 90% was reached at levels of cold SLG of 0.3–0.6 μg. The lack of complete inhibition of binding suggests the occurrence of a small degree of non-specific cellular association. SL pre-incubated with cells under the same conditions did not interfere with the cellular association of SLG (data not shown).

Overall, these data suggest that the peptide-specific and cell-specific interactions between SLG and the H69 cell line, where binding and endocytosis of liposomes take place, was mainly governed by a receptor-mediated process, through the formation of clathrin-coated pits.

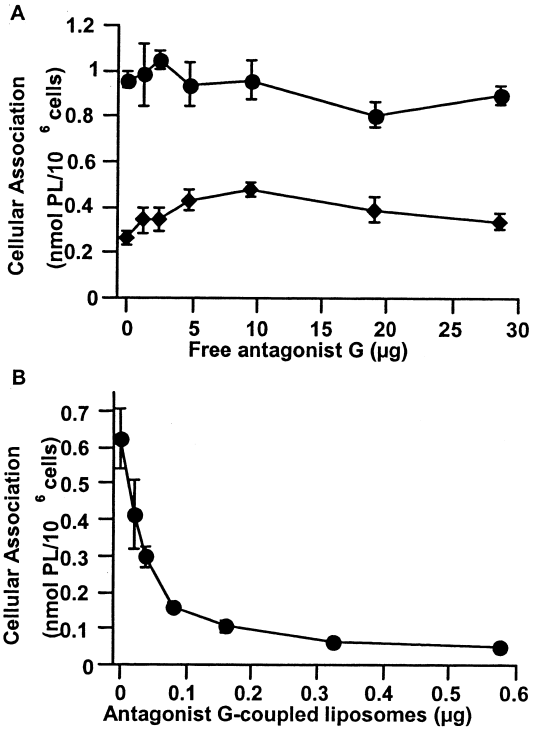

Fig. 3. Competitive inhibition of cellular association of [^{3}H]CHE-SLG in SCLC H69. One million SCLC H69 cells were first incubated for 30 min with either (A) 0–29 μg of free antagonist G, either at 4°C (♦) or 37°C (●) or (B) 0–0.6 μg of coupled antagonist G on non-radiolabeled SLG at 37°C (●). Inhibition was determined by adding [^{3}H]CHE-SLG (0.1 mM PL/well), either at 4°C or 37°C for 1 h. The cells were then washed with cold PBS. Cellular association of liposomes was expressed as nmol of PL/10^6 cells. Each point is the mean of three samples, ± standard deviation, from one representative experiment.

The mechanism of action of antagonist G is still unclear; however, it is believed that it interacts with receptors on the cell surface in a dose dependent manner, competing with neuropeptide growth factors produced by SCLC cells [6,8]. To test whether the cellular association of SLG would be competitively inhibited by neuropeptide growth factors, H69 cells were incubated with conditioned media [49,50] (RPMI 1640 supplemented with 10% (v/v) heat-inactivated FBS, 100 U/ml penicillin and 100 μg/ml streptomycin that had been incubated with the cells at 37°C for 3 days). Cellular association of SLG decreased only slightly in the presence of conditioned media (Fig. 4).

2.2. DXR uptake kinetics

The nucleus, with its high DNA content, is an important intracellular target for DXR. To compare the efficiency of cellular delivery of DXR for targeted versus non-targeted formulations, the uptake kinetics of DXR into whole cells or isolated nuclei was studied at 37°C for 24 h in the H69 cell line. In whole cells, uptake of free DXR was, as expected, rapid and high levels were obtained, since there is no redistribution phenomenon to lower drug levels in cell culture, unlike the in vivo situation for the free drug. Uptake by cells of DXR in SLG, although not to as high levels as free DXR, was significantly faster and to higher levels than drug delivered by SL or SLP(1–9) (Fig. 5A). After 6 h of incubation, the amount of DXR delivered by SLG was more than 35 times higher than the amount delivered by SL. Not unexpectedly, the kinetics of nuclear uptake of DXR, either free or liposomal, was slower than that for whole cells and the levels of maximum uptake were lower (Fig. 5B). DXR delivered to nuclei by SLG was lower than that for free DXR, and the rate of nuclear accumulation of drug was slower (Fig. 5B). However, after 6 h of incubation, the amount of DXR delivered by SLG was more than 140-fold higher than the amount delivered by SL. In all cases, drug uptake of free DXR and SLG appeared to saturate by around 12 h, but uptake continued to increase for SL and SLP(1–9), likely due to continued extracellular release of drug from the liposomes. These data support the hypothesis that liposomal

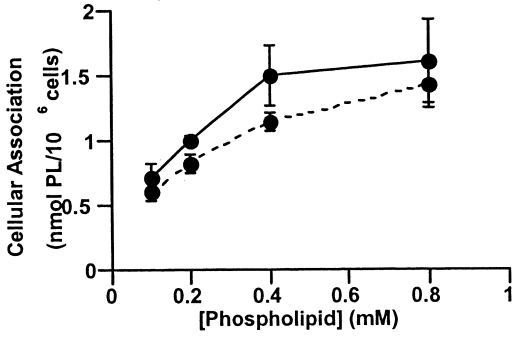

Fig. 4. Cellular association of [^{3}H]CHE-SLG to H69 cells in full versus conditioned media. Liposomes composed of HSPC/CHOL/mPEG$_{2000}$-DSPE/PDP-PEG$_{2000}$-DSPE at a 2:1:0.08:0.02 molar ratio, with coupled antagonist G (0.1–0.8 mM PL/well), were incubated with 1×10^6 H69 cells at 37°C for 1 h, with full (●) or 3-day conditioned media (●). After washing with cold PBS, the amount of [^{3}H]CHE-liposomes associated with cells was determined by scintillation counting and it was calculated from the initial specific activity of [^{3}H]CHE-liposomes. Data was expressed as nmol of PL/10^6 cells. Each point is the mean of three samples, ± standard deviation, from one representative experiment.

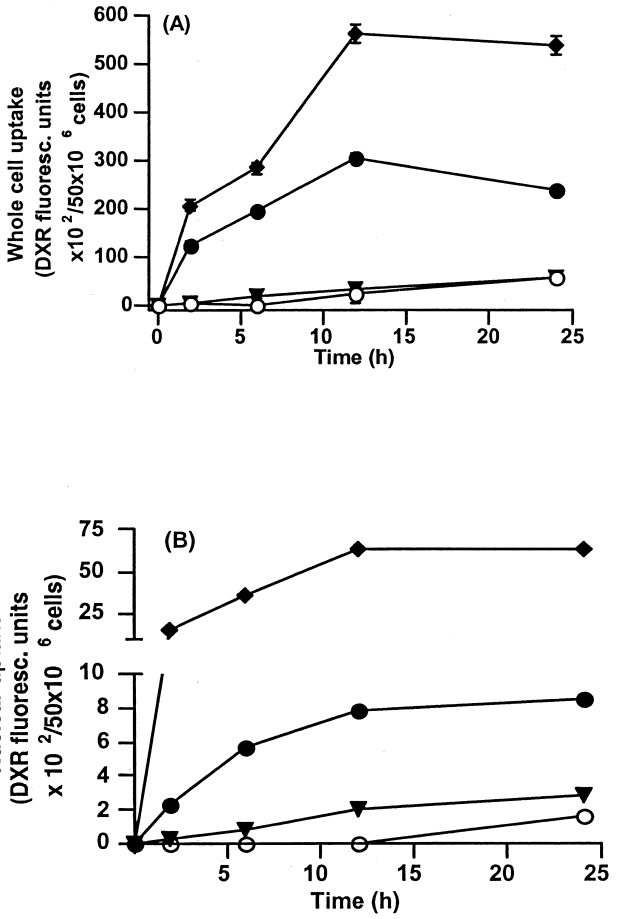

Fig. 5. Kinetics of uptake of DXR or DXR-containing liposomes by H69 cells. Twenty μM of free DXR (♦) or DXR-containing liposomes composed of HSPC/CHOL/mPEG$_{2000}$-DSPE/PDP-PEG$_{2000}$-DSPE at a 2:1:0.08:0.02 molar ratio (DXR-SL, ○; DXR-SLG, ●; and DXR-SLP(1–9), ▼), were incubated with 50×10^6 SCLC H69 cells at 37°C for 24 h. After each time point, cells were washed and resuspended in TEA buffer. Aliquots were taken to determine DXR accumulation in whole cells. The remaining cells were ruptured and the nuclear fraction was isolated. Following enzymatic digestion to recover DNA-bound drug, DXR was measured in whole cell extracts (A) or in the isolated nuclei (B). Background was subtracted from the values in each time point and the results were expressed as DXR fluorescence units/50×10^6 cells. Each point is the mean of three samples, ± standard deviation, from one representative experiment.

drugs, targeted against internalizing receptors, cannot only increase the selective uptake of drug by target cells but also result in drug release from the endosomal compartments allowing the drug to reach intracellular sites of action.

2.3. Cytotoxicity

Cytotoxicity of DXR-SL, DXR-SLG, SLG without DXR, free DXR with or without empty SLG, and free antagonist G was tested for 2, 24 and 48 h incubations against the H69 cell line (Table 1). For both 2-h and 24-h incubation periods, the cytotoxicity of DXR-SLG was approximately 20-fold higher than DXR-SL ($P < 0.001$), and it remained higher (9-fold) even after 48 h of incubation ($P < 0.001$), where release and uptake of drug from the non-targeted liposomes would be expected to be high. The targeted formulation was much faster in triggering a cytotoxic effect, taking 2–24 h to reach its maximum effect. After 48 h, the cytotoxicity of DXR-SL was still 3-fold lower than the cytotoxicity of DXR-SLG after 2 h ($P < 0.01$). Due to the rapid diffusion through cell membranes of free DXR [51], its cytotoxicity after a 2-h incubation was approximately 4-fold higher than DXR-SLG ($P < 0.001$). However, after 24 and 48 h the differences were no longer statistically significant ($P > 0.05$). At all time points, DXR-SL was always significantly less cytotoxic than the free drug ($P < 0.001$). The high IC_{50} (1000 μM PL) for empty SLG suggests that neither the coupled antagonist G nor the lipid, nor the combination of the two, contributed to the cytotoxic effect observed for DXR-containing SLG (at the IC_{50} the concentration of PL is approximately 10–30 μM). The cytotoxicity of free antagonist G was significantly lower than that for free DXR or DXR-SLG ($P < 0.001$) at all time points. Moreover, the similar IC_{50}s for free DXR and free DXR plus empty SLG ($P > 0.05$) suggests that there was no synergistic effect between free DXR and/or lipid and/or coupled peptide.

The Namalwa cell line, a negative control in these experiments, was as sensitive to free DXR as the H69 cell line at all incubation periods. As expected, the IC_{50}s of DXR-SL and DXR-SLG against the Namalwa cell line were not significantly different at any time point ($P > 0.05$), as this cell line does not have receptors that specifically recognize antagonist G.

2.4. Pharmacokinetics and biodistribution of liposomes

The pharmacokinetics and biodistribution of SL and SLG were evaluated in outbred female CD_1(ICR)BR mice with [^{125}I]TI-containing liposomes. The [^{125}I]TI is an excellent marker for intact liposomes as the label is metabolically inert and, when released from liposomes by body fluids, is rapidly eliminated from the body via kidney filtration [36]. The data are presented as percentage of in vivo cpm, which corrects for leakage of the label and represents intact liposomes remaining in the body at the given time points [19].

SL and SLG had mean residence times (MRT) of

Table 2
Pharmacokinetic parameters of SLG or SL in CD_1(ICR)BR mice

Sample	MRT[a] (h)	AUC[b] (nmol h/ml)	k_{10}[c] (h^{-1})	$T_{1/2}\alpha$[d] (h)	$T_{1/2}\beta$[e] (h)
SL	25.2	10925	0.046	0.0544	17.46
SLG	18.4	4887	0.10	0.303	13.04

Liposomes, composed of HSPC/CHOL/mPEG$_{2000}$-DSPE/PDP-PEG$_{2000}$-DSPE at a 2:1:0.08:0.02 molar ratio, with or without coupled antagonist G, and containing the aqueous-space label [^{125}I]TI, were injected via the tail vein as a single bolus dose (0.5 μmol PL/mouse). At different times post-injection, up to 48 h, major organs and blood were collected and counted for ^{125}I label. Pharmacokinetic parameters were calculated using polyexponential curve stripping and the least squares parameter estimation program, PKAnalyst 1.0.

[a]Mean residence time.

[b]Area under the blood concentration versus time curve.

[c]Elimination rate constant from the central compartment.

[d]$T_{1/2}\alpha$, half-life for initial elimination phase.

[e]$T_{1/2}\beta$, half-life for terminal elimination phase.

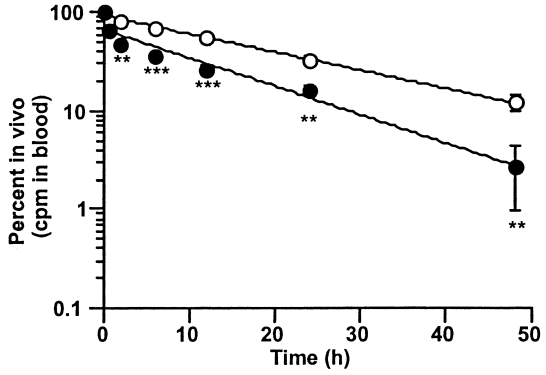

Fig. 6. Blood clearance kinetics of SLG or SL in CD_1(ICR)BR mice. Liposomes composed of HSPC/CHOL/mPEG$_{2000}$-DSPE/PDP-PEG$_{2000}$-DSPE at 2:1:0.08:0.02 molar ratio, with (●) or without coupled antagonist G (○), and containing the aqueous-space label [^{125}I]TI, were injected via the tail vein with a single bolus dose (0.5 μmol PL/mouse). At different times post-injection major organs and blood were collected and counted for ^{125}I label. Results were expressed as the percentage of counts in the blood relative to the total counts remaining in vivo at each time point. Each point represents the average of three mice, ± standard deviation (**$P < 0.005$; ***$P < 0.0005$).

25.2 and 18.4 h, respectively (Table 2). SL were cleared from the blood mainly in a log-linear single exponential process (Fig. 6 and Table 2), whereas SLG were cleared in a biphasic manner, characterized by two elimination half-lives, $T_{1/2}\alpha$ and $T_{1/2}\beta$ (Fig. 6 and Table 2), most likely due to a relatively high spleen uptake of a portion of the SLG shortly after intravenous injection (Table 3). SLG had an area under the blood concentration versus time curve (AUC) of 4887 nmol h/ml, which was approximately half that for SL (10924 nmol h/ml), and an increased elimination rate constant, k_{10} from the central compartment (Table 2). One half hour after injection, the blood levels of SLG had dropped to 65%, due primarily to splenic clearance (19%), which was high compared to liver clearance (4.5%) at the same time point (data not shown). Nevertheless, the clearance kinetics of both samples were dominated by $T_{1/2}\beta$. SLG had a long-circulating blood clearance profile similar to that of other PEG-grafted liposomes (Fig. 6) that are long-circulating [19].

The 2-h and 24-h biodistribution of both SLG and SL is reported in Table 3. Uptake into lung, heart and kidney of either SLG or SL was low, as was spleen uptake of SL. Carcass uptake was higher for SL than for SLG at 24 h, likely a result of the higher spleen levels of SLG. The cause for the high spleen uptake of SLG relative to SL is not known, but some specific binding of antagonist G in the spleen may be occurring.

3. Discussion

SCLC has the highest metastatic potential of any solid tumor, with more than 90% of patients having widespread metastases at presentation [2]. SCLC secretes multiple neuropeptides growth factors whose receptor-mediated actions can be inhibited by several peptide antagonists [4]. Hence, peptide antagonist-targeted, internalized, liposomal delivery systems have the potential to improve treatment of this disease. In this paper we have demonstrated that antagonist G-targeted liposomes are specifically recognized and internalized by a SCLC cell line, H69, through a receptor-mediated process, which leads to intracellu-

Table 3
Tissue distributions of SLG or SL in CD_1(ICR)BR mice

Sample	Blood	Liver	Spleen	Lung	Heart	Kidney	Carcass
2 h post dose							
SL	79.53 ± 5.86	4.61 ± 1.16	0.06 ± 0.08	0.25 ± 0.25	0.36 ± 0.07	1.91 ± 0.39	13.17 ± 5.23
SLG	47.43 ± 2.81	8.42 ± 1.59	25.60 ± 2.94	0.81 ± 0.14	0.64 ± 0.09	1.10 ± 0.09	15.99 ± 5.18
24 h post dose							
SL	32.67 ± 2.93	16.45 ± 1.99	1.65 ± 0.24	0.38 ± 0.21	0.66 ± 0.06	3.71 ± 0.28	43.81 ± 4.04
SLG	15.91 ± 1.86	25.29 ± 1.90	30.49 ± 2.26	0.43 ± 0.04	0.36 ± 0.04	1.93 ± 0.38	25.51 ± 1.83

Liposomes, composed of HSPC/CHOL/mPEG$_{2000}$-DSPE/PDP-PEG$_{2000}$-DSPE at a 2:1:0.08:0.02 molar ratio, with or without coupled antagonist G, and containing the aqueous-space label [^{125}I]TI, were injected via the tail vein as a single bolus dose (0.5 μmol PL/mouse). At different times post-injection, major organs and blood were collected and counted for ^{125}I label. Results were expressed as the percentage of counts in each organ relative to the total counts remaining in vivo at each time point. Each point represents the average of three mice ± standard deviation.

lar drug accumulation and release to intracellular sites of action, resulting in cytotoxicity. The targeted liposomes are long-circulating, which is a necessary property for in vivo applications [14].

Although it was beyond the scope of the present work to identify the receptor(s) that mediated internalization of SLG, it has been previously shown that antagonist G had a high affinity for the vasopressin receptor [6], which is widely expressed in SCLC tumors [52]. In several cell lines, vasopressin receptors have been described as being internalizing (although it depends on the particular ligand [53]) via a clathrin-coated pit mediated process [54–56], with the ability to recycle back to the cell surface at different rates depending on the vasopressin receptor subtype [57–59]. The ability of targeted liposomes to trigger receptor-mediated endocytosis is thought to be important for the cytotoxicity of their entrapped drugs [29], although the binding of targeted liposomes is not always followed by liposome endocytosis [60,61].

From the binding results at 4°C and 37°C (Fig. 1A), based on the assumption that the number of liposomes/μmol PL was 7.7×10^{12} [29], a maximum number of approximately 13,000 SLG were internalized/cell after a 1 h incubation at 37°C. This value was 4.8-fold higher than the one obtained for the same initial PL concentration for 1 h incubation at 4°C, which is non-permissive for endocytosis [25]. This suggests that following binding of SLG, the target receptor is internalized (likely via the clathrin coated-pit pathway, Fig. 1C) and then rapidly recycled back to the cell surface where it is then available to bind and internalize more SLG. Under our experimental conditions, with increasing PL concentrations (0.1–0.8 mM), the target receptor may take about 7–13 min to be recycled. Therefore, there are some similarities between this receptor and vasopressin receptors, described in the previous paragraph. Further evidence to support the endocytosis of SLG comes from the intracellular fluorescence observed in confocal experiments (Fig. 2A). As expected, the cellular association of SL, which is neutrally charged and lacks associated ligands, was only 3–5% of that seen for SLG cellular association (Fig. 1A). Competition data (Fig. 3B) provided additional confirmation that SLG internalization was receptor-mediated.

As mentioned before, antagonist G antiproliferative activity is mediated primarily by its competitive inhibition of the binding of several growth factors produced by SCLC cells [6,8]. The receptor binding takes place through the hydrophobic residues 7–10 [6]. Inhibition of binding of radiolabeled SLG by cold antagonist G-coupled liposomes, but not by free antagonist G (neither at 37 nor at 4°C), suggests that multivalent binding sites may be involved in the binding (Fig. 3B). Coupling of peptide to liposomes would change the avidity of the receptor binding, by allowing a multivalent presentation of the peptide. Changes in the orientation and/or mobility of the liposomal peptide, compared to free peptide, may also contribute to differences between free peptide and liposome-coupled peptide in the competition experiments. The immobilization of small peptides on liposome surfaces has been shown to be a useful approach, for example, in the designing of synthetic vaccines [62] and in the suppression of tumor metastasis [63]. The inhibition of E-selectin-mediated cellular adhesion in inflammatory processes has also been dramatically improved by the attachment, at the end of PEG-grafted liposomes, of the oligosaccharide sialyl Lewis^X, recognized by E-selectin [64]. The present data suggested that liposomal presentation might be an effective means of improving the performance of broad-spectrum neuropeptide antagonists against SCLC and this strategy deserves further investigation.

The rate and extent of uptake of DXR was higher for SLG than for non-targeted formulations (Fig. 5A,B), although not as rapid as that seen for free DXR. Although free DXR has an advantage in cell culture, due to its ability to passively diffuse through cell membranes [51], this advantage will be lost in vivo due to the rapid drop in plasma levels of free DXR as a consequence of the redistribution of the drug to tissues [15]. The relative advantage of targeted liposomal formulations of DXR relative to free drug in vivo, has been demonstrated for anti-CD19-targeted liposomal DXR in the treatment of xenograft models of B lymphoma [29].

The amount of DXR-SLG in the whole cell and its rate of accumulation were faster than in isolated nuclei. Several factors come into play here. The amount of DXR associated with whole cells may be overestimated due to (1) contributions from non-specifically

adsorbed liposomes on the cell surface, (2) uptake of free drug that was released from the SLG prior to internalization, and (3) drug present in bound, non-internalized, liposomes. Drug associated with isolated nuclei could come from either uptake of drug released at the cell surface that subsequently trafficked to the nucleus, or to drug that was internalized in SLG, was released from the endosomes and then trafficked to the nucleus. It is believed that, once DXR-SLG reaches the endosomes, bilayer damage by the enzymatic activity of phospholipases will destroy the proton gradient in the liposomes, leading to DXR release [65]. The amount of nuclear accumulation of DXR contributed from drug released from liposomes at the cell surface can be approximated from the data for non-targeted liposomes (DXR-SL). Since the levels of DXR in nuclei for DXR-SL are very low relative to DXR-SLG, we can conclude that the majority of DXR in the nuclei in cells exposed to DXR-SLG comes from internalized liposomes that have released their contents from the lysosomal apparatus. Based on the binding data presented before (Fig. 1A), and assuming an average amount of DXR per liposome of 200 μg/μmol PL, SLG delivered approximately $100–430 \times 10^6$ DXR molecules/cell, which emphasizes the great potential of this strategy for intracellular delivery of large payloads.

The increased levels of cellular and nuclear DXR for DXR-SLG compared to DXR-SL led to increased cytotoxicity (Table 1). With increasing incubation times the differences in cytotoxicity between SLG and SL tended to decrease, confirming observations from other authors [29,65]. With increasing incubation times, the amount of drug released from liposomes either non-specifically adsorbed to the cell surface or in the media will increase, and the released (free) drug will make a larger contribution to cytotoxicity at longer time points. The results obtained with the H69 cell line, compared to the Namalwa cell line, suggest that cell surface receptors that specifically recognize antagonist G are involved in the cytotoxicity of DXR-SLG.

Long circulation times are required for liposomes to gain access to tumor sites [14,15,66]. Although SLG (1 nmol antagonist G/μmol PL) were removed more rapidly from circulation than SL due to a component of splenic uptake, nevertheless SLG still had blood clearance profiles typical of long circulating formulations when compared to non-PEGylated formulations, which are rapidly removed from circulation after injection [19]. Another study has shown that PEG-grafted liposomes, having the pentapeptide H-Tyr-Ile-Gly-Ser-Arg-NH_2 (2.6 and 7.3 nmol of peptide/μmol PL) attached at the PEG terminus, had low blood clearance rates [67]. Interestingly, targeted liposomes made with whole antibodies, e.g., 1 nmol of sheep IgG/μmol PL [27] or 0.7 nmol of N-12A5/μmol PL [61], were rapidly removed from the circulation. These data suggest that liposomes are able to carry much higher concentrations of smaller ligands like peptides without losing their long circulating properties. Thus, the covalent attachment of small, therapeutically active peptides to the terminus of liposomal surface-grafted PEG chains, might improve the therapeutic efficacy of targeted liposomes [67].

The distribution of SLG is very different from that of free antagonist G, which has the liver as the main site of accumulation [11]. PEG-grafted liposomes like those used in our experiments (100–130 nm in diameter) have low hepatosplenic uptake [68]. We hypothesize that antagonist G stimulated the vasopressin receptor-mediated splenic uptake of SLG, as it is known that vasopressin receptors are expressed in the spleen [69,70].

In summary, our results suggest that antagonist G-targeted liposomes are a promising vehicle for the delivery of chemotherapeutic drugs and gene therapeutics, e.g., antisense oligonucleotides, for the treatment of human small cell lung cancer. This needs to be confirmed in vivo in appropriate model systems, and such experiments are under way.

Acknowledgements

J.N.M. was the recipient of a Portuguese grant from Praxis XXI (Ref.: BD/5600/95). The technical assistance of Susan Cubitt and Elaine Moase was greatly appreciated. The authors would like to thank Dr. M.J. Kirchmeier for helping with DXR uptake kinetic experiments and Dr. Xuejun Sun for suggestions on confocal experiments, which took place at the Department of Oncology, Cross Cancer Institute, Edmonton, Canada.

References

[1] A.C. MacKinnon, R.A. Armstrong, C.M. Waters, J. Cummings, J.F. Smyth, C. Haslett, T. Sethi, Br. J. Cancer 80 (1999) 1026–1034.
[2] S.M. Moore, R.C. Rintoul, T.R. Walker, E.R. Chilvers, C. Haslett, T. Sethi, Cancer Res. 58 (1998) 5239–5247.
[3] D.A. Jones, J. Cummings, S.P. Langdon, J.F. Smyth, Gen. Pharmacol. 28 (1997) 183–189.
[4] T. Sethi, S. Langdon, J. Smyth, E. Rozengurt, Cancer Res. 52s (1992) 2737s–2742s.
[5] P.J. Woll, E. Rozengurt, Proc. Natl. Acad. Sci. USA 85 (1988) 1859–1863.
[6] P.J. Woll, E. Rozengurt, Cancer Res. 50 (1990) 3968–3973.
[7] P.A. Bunn Jr., D. Chan, J. Stewart, L. Gera, R. Tolley, P. Jewett, M. Tagawa, C. Alford, T. Mochzuki, N. Yanaihara, Cancer Res. 54 (1994) 3602–3610.
[8] M.J. Seckl, R.H. Newman, P.S. Freemont, E. Rozengurt, J. Cell. Physiol. 163 (1995) 87–95.
[9] D.A. Jones, J. Cummings, S.P. Langdon, A.J. MacLellan, T. Higgins, E. Rozengurt, J.F. Smyth, Peptides 16 (1995) 777–783.
[10] D.A. Jones, J. Cummings, S.P. Langdon, A. Maclellan, J.F. Smyth, Biochem. Pharmacol. 50 (1995) 585–590.
[11] J. Cummings, A.J. MacLellan, D.A. Jones, S.P. Langdon, E. Rozengurt, A.A. Ritchie, J.F. Smyth, Ann. Oncol. 6 (1995) 595–602.
[12] S. Langdon, T. Sethi, A. Ritchie, M. Muir, J. Smyth, E. Rozengurt, Cancer Res. 52 (1992) 4554–4557.
[13] R.L. Comis, D.M. Friedland, B.C. Good, Oncology 12 (1998) 44–50.
[14] D. Papahadjopoulos, T.M. Allen, A. Gabizon, E. Mayhew, K. Matthay, S.K. Huang, K.D. Lee, M.C. Woodle, D.D. Lasic, C. Redemann, F.J. Martin, Proc. Natl. Acad. Sci. USA 88 (1991) 11460–11464.
[15] A. Gabizon, R. Catane, B. Uziely, B. Kaufman, T. Safra, R. Cohen, F. Martin, A. Huang, Y. Barenholz, Cancer Res. 54 (1994) 987–992.
[16] D.D. Lasic, F.J. Martin, A. Gabizon, S.K. Huang, D. Papahadjopoulos, Biochim. Biophys. Acta 1070 (1991) 187–192.
[17] A.L. Klibanov, K. Maruyama, V.P. Torchilin, L. Huang, FEBS Lett. 268 (1990) 235–237.
[18] T.M. Allen, C. Hansen, F. Martin, C. Redemann, A. Yau-Young, Biochim. Biophys. Acta 1066 (1991) 29–36.
[19] T.M. Allen, C. Hansen, Biochim. Biophys. Acta 1068 (1991) 133–141.
[20] F.J. Martin, Oncology 11 (1997) 11–20.
[21] F.M. Muggia, Drugs 54 (1997) 22–29.
[22] G. Blume, G. Cevc, M.D. Crommelin, I.A. Bakker-Woudenberg, C. Kluft, G. Storm, Biochim. Biophys. Acta 1149 (1993) 180–184.
[23] K. Maruyama, T. Takizawa, T. Yuda, S.J. Kennel, L. Huang, M. Iwatsuru, Biochim. Biophys. Acta 1234 (1995) 74–80.
[24] D.E. Lopes de Menezes, M.J. Kirchmeier, J.F. Gagne, L.M. Pilarski, T.M. Allen, J. Liposome Res. 9 (1999) 199–228.
[25] R.J. Lee, P.S. Low, J. Biol. Chem. 269 (1994) 3198–3204.
[26] C.B. Hansen, G.Y. Kao, E.H. Moase, S. Zalipsky, T.M. Allen, Biochim. Biophys. Acta 1239 (1995) 133–144.
[27] T.M. Allen, E. Brandeis, C.B. Hansen, G.Y. Kao, S. Zalipsky, Biochim. Biophys. Acta 1237 (1995) 99–108.
[28] I. Ahmad, M. Longenecker, J. Samuel, T.M. Allen, Cancer Res. 53 (1993) 1484–1488.
[29] D.E. Lopes de Menezes, L.M. Pilarski, T.M. Allen, Cancer Res. 58 (1998) 3320–3330.
[30] N. Shi, W.M. Pardridge, Proc. Natl. Acad. Sci. USA 97 (2000) 7567–7572.
[31] G. Pagnan, D.D. Stuart, F. Pastorino, L. Raffaghello, P.G. Montaldo, T.M. Allen, B. Calabretta, M. Ponzoni, J. Natl. Cancer Inst. 92 (2000) 253–261.
[32] J.A. Harding, C.M. Engbers, M.S. Newman, N.I. Goldstein, S. Zalipsky, Biochim. Biophys. Acta 1327 (1997) 181–192.
[33] D. Kirpotin, J.W. Park, K. Hong, S. Zalipsky, W.L. Li, P. Carter, C.C. Benz, D. Papahadjopoulos, Biochemistry 36 (1997) 66–75.
[34] J.W. Park, K. Hong, P. Carter, H. Asgari, L.Y. Guo, G.A. Keller, C. Wirth, R. Shalaby, C. Kotts, W.I. Wood, D. Papahadjopoulos, C.C. Benz, Proc. Natl. Acad. Sci. USA 92 (1995) 1327–1331.
[35] J.W. Park, K. Hong, D.B. Kirpotin, D. Papahadjopoulos, C.C. Benz, Adv. Pharmacol. 40 (1997) 399–435.
[36] E.F. Sommerman, P.H. Pritchard, P.R. Cullis, Biochem. Biophys. Res. Commun. 122 (1984) 319–324.
[37] D.L. Daleke, K. Hong, D. Papahadjopoulos, Biochim. Biophys. Acta 1024 (1990) 352–366.
[38] S. Zalipsky, C.B. Hansen, J.M. Oaks, T.M. Allen, J. Pharm. Sci. 85 (1996) 133–137.
[39] F. Olson, C.A. Hunt, F.C. Szoka, W.J. Vail, D. Papahadjopoulos, Biochim. Biophys. Acta 557 (1979) 9–23.
[40] E.M. Bolotin, R. Cohen, L.K. Bar, N. Emanuel, S. Ninio, D.D. Lasic, Y. Barenholz, J. Liposome Res. 4 (1994) 455–479.
[41] K. Fujiwara, Y. Motomi, T. Kitagawa, J. Immunol. Methods 45 (1981) 195–203.
[42] G.R. Bartlett, J. Biol. Chem. 234 (1959) 466–468.
[43] J.G. Reeve, N.M. Bleehen, Biochem. Biophys. Res. Commun. 199 (1994) 1313–1319.
[44] M.J. Kirchmeier, T. Ishida, J. Chevrette, T.M. Allen, J. Liposome Res. 11 (2001) 15–29.
[45] T. Mosmann, J. Immunol. Methods 65 (1983) 55–63.
[46] J.E. Heuser, R.G. Anderson, J. Cell Biol. 108 (1989) 389–400.
[47] O. Zelphati, F.C. Szoka Jr., Pharm. Res. 13 (1996) 1367–1372.
[48] H. Matsui, L.G. Johnson, S.H. Randell, R.C. Boucher, J. Biol. Chem. 272 (1997) 1117–1126.
[49] G.D. Sorenson, O.S. Pettengill, T. Brinck-Johnsen, C.C. Cate, L.H. Maurer, Cancer 47 (1981) 1289–1296.
[50] J.E. Layton, D.B. Scanlon, C. Soveny, G. Morstyn, Cancer Res. 48 (1988) 4783–4789.

[51] R. Regev, G.D. Eytan, Biochem. Pharmacol. 54 (1997) 1151–1158.
[52] W.G. North, M.J. Fay, K.A. Longo, J. Du, Cancer Res. 58 (1998) 1866–1871.
[53] W. Lutz, J.M. Londowski, M. Sanders, J. Salisbury, R. Kumar, J. Biol. Chem. 267 (1992) 1109–1115.
[54] B. Hocher, H.J. Merker, J.A. Durr, S. Schiller, P. Gross, J. Hensen, Biochem. Biophys. Res. Commun. 186 (1992) 1376–1383.
[55] R. Pfeiffer, J. Kirsch, F. Fahrenholz, Exp. Cell Res. 244 (1998) 327–339.
[56] W. Lutz, M. Sanders, J. Salisbury, S. Lolait, A.M. O'Carroll, R. Kumar, Kidney Int. 43 (1993) 845–852.
[57] G. Innamorati, H.M. Sadeghi, N.T. Tran, M. Birnbaumer, Proc. Natl. Acad. Sci. USA 95 (1998) 2222–2226.
[58] G. Innamorati, H. Sadeghi, M. Birnbaumer, J. Biol. Chem. 273 (1998) 7155–7161.
[59] R.H. Oakley, S.A. Laporte, J.A. Holt, L.S. Barak, M.G. Caron, J. Biol. Chem. 274 (1999) 32248–32257.
[60] U.K. Nässander, P.A. Steerenberg, H. Poppe, G. Storm, L.G. Poels, W.H. De Jong, D.J. Crommelin, Cancer Res. 52 (1992) 646–653.
[61] D. Goren, A.T. Horowitz, S. Zalipsky, M.C. Woodle, Y. Yarden, A. Gabizon, Br. J. Cancer 74 (1996) 1749–1756.
[62] M. Friede, S. Muller, J.P. Briand, M.H. Van Regenmortel, F. Schuber, Mol. Immunol. 30 (1993) 539–547.
[63] M. Takikawa, H. Kikkawa, T. Asai, N. Yamaguchi, D. Ishikawa, M. Tanaka, K. Ogino, T. Taki, N. Oku, FEBS Lett. 466 (2000) 381–384.
[64] S.A. DeFrees, L. Phillips, L. Guo, S. Zalipsky, J. Am. Chem. Soc. 118 (1996) 6101–6104.
[65] D. Goren, A.T. Horowitz, D. Tzemach, M. Tarshish, S. Zalipsky, A. Gabizon, Clin. Cancer Res. 6 (2000) 1949–1957.
[66] A. Gabizon, D. Papahadjopoulos, Proc. Natl. Acad. Sci. USA 85 (1988) 6949–6953.
[67] S. Zalipsky, B. Puntambekar, P. Boulikas, C.M. Engbers, M.C. Woodle, Bioconjug. Chem. 6 (1995) 705–708.
[68] D.C. Litzinger, A.M. Buiting, N. van Rooijen, L. Huang, Biochim. Biophys. Acta 1190 (1994) 99–107.
[69] J. Elands, A. Resink, E.R. De Kloet, Endocrinology 126 (1990) 2703–2710.
[70] S.J. Lolait, A.M. O'Carroll, L.C. Mahan, C.C. Felder, D.C. Button, W.S. Young III, E. Mezey, M.J. Brownstein, Proc. Natl. Acad. Sci. USA 92 (1995) 6783–6787.